

Structural Characterization of *anti*- and *syn*-Allyltricarboxyliron Bromide: Rotational Spectra, Quadrupole Coupling, and Density Functional Calculations

Brian J. Drouin,[†] Jennifer J. Dannemiller, and Stephen G. Kukolich*

Department of Chemistry, University of Arizona, Tucson, Arizona 85721

Received July 26, 1999

Rotational transitions for two distinct structural isomers of allyltricarboxyliron bromide have been clearly observed in the cold molecular beam of a pulsed-beam Fourier transform microwave spectrometer. Rotational transitions exhibiting quadrupole splitting patterns for each isomer were measured for the ⁷⁹Br and ⁸¹Br isotopomers. Both isomers are accidental near-prolate symmetric tops. The measured rotational constants for the ⁷⁹Br isotopomer are $A(\text{anti}) = 920.6148(2)$ MHz, $B(\text{anti}) = 582.8866(12)$ MHz, $C(\text{anti}) = 581.3027(12)$ MHz, $A(\text{syn}) = 919.5055(1)$ MHz, $B(\text{syn}) = 584.1865(1)$ MHz, and $C(\text{syn}) = 581.6392(1)$ MHz. Analysis of the isotopic substitution data and possible transition assignments indicates that these molecules have C_s symmetry. Both isomers are found to have a dipole component along the a axis. However, the anti isomer has a “ c ” type dipole component, whereas a “ b ” dipole component is found for the syn isomer. It was found necessary to carefully analyze both rotational constants and the quadrupole coupling data in order to determine the correct assignment of dipole moment components for each isomer. This change in dipole assignments implies that there is a switch of inertial axes upon isomerization resulting from a subtle shift of the allyl center of mass coordinates, upon reorientation of the allyl ligand. The X-ray and DFT calculated structures for the anti isomer are in excellent agreement with the present data. No previous structural data for the syn isomer were available, and the present analysis strongly supports the expected conformation.

Introduction

There has been much continued interest in the allyl ligand in organometallic chemistry due to its special property of being a small resonance stabilized ligand. This ligand, formally a three-electron π donor, has been shown to form stable compounds with a wide variety of metal centers. The π -donor three-electron bond is particularly interesting in mechanistic studies since intermediate species in reactions of olefins may be stabilized by such an interaction. For example, olefin isomerization on a metal center typically begins (and ends) with temporary coordination of the two olefinic carbons to the metal center. The isomerization process then proceeds through intermediate structures with either single carbon coordination or three-center (allylic) coordination.¹ A similar allylic intermediate is believed to exist during the catalytic carbonylation of allylic halides.²

The allyl ligand is often weakly bound and can exhibit internal rotation with barriers on the order of ~ 4 kcal mol⁻¹. Crystal structures usually exhibit only the lowest energy conformation of the complex, and the one isomer observed in the X-ray work³ corresponds to the *anti*-allyltricarboxyliron bromide isomer shown in Figure 1. We have designated the isomer with the central carbon atom farthest from the bromine atom as the anti isomer. We believe that the anti and syn designations are less ambiguous and more appropriate for this organometallic complex. Two isomers have been identified in solution using standard NMR techniques. The dynamics of allyl ligand

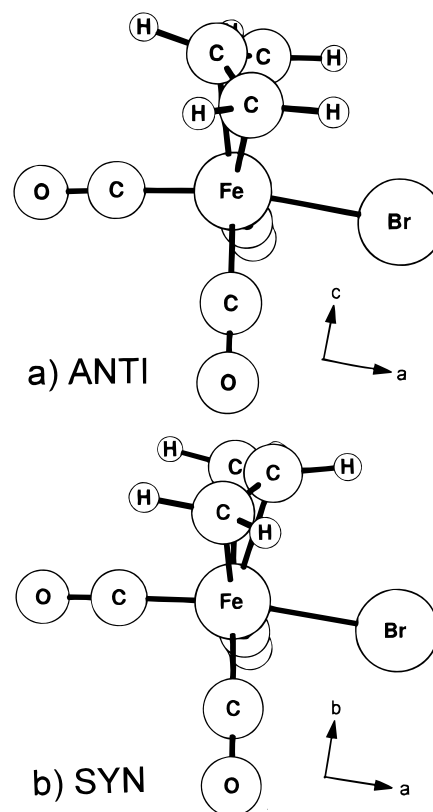


Figure 1. Basic structures for (a) *anti*- and (b) *syn*-allyltricarboxyliron bromide. The a , c principal inertial axes are indicated for anti, and a , b principal inertial for syn isomers.

rearrangement mechanisms have been studied using NMR methods. For molecules of the type $C_3H_5Fe(CO)_3X$, $X = NO_3$,

[†] Present address: Jet Propulsion Lab., 4800 Oak Grove Dr., Pasadena, CA 91109-8099.

- (1) Crabtree, R. H. *The Organometallic Chemistry of the Transition Metals*; Wiley-Interscience Inc.: New York, 1994; Chapter 9.
- (2) Dent, W. T.; Long, R.; Wilkinson, A. J. *J. Chem. Soc.* **1964**, 1585 and 1588. See also: Cotton, F. A.; Wilkinson, G. *Advanced Inorganic Chemistry*, 2nd ed.; John Wiley: New York, 1966; p 785.
- (3) Simon, F. E.; Lauher, J. W. *Inorg. Chem.* **1980**, *19*, 2338.

Cl, Br, I, and C₃H₅, the variable-temperature NMR data⁴ show that decreasing electronegativity of the ligand causes a corresponding decrease in the barrier to internal rotation. The NMR study of Nesmeyonov⁴ also included a semiempirical Hückel treatment that suggests the allyl ligand in the syn isomer is less tightly bound than in the anti isomer. A high-resolution IR study and structural parameters of the free allyl radical were reported by Hirota et al.⁵

In the present analysis, microwave spectra provide gas-phase evidence for two structural isomers of allyltricarbylironbromide. The resulting structural data are in agreement with solid-state data³ for the anti isomer. DFT calculations provide structural parameters for the carbonyl and allyl portions of the molecule, which are in good agreement with the present and previous studies. The new, high-resolution spectra allow accurate measurements of the bromine quadrupole coupling parameters. The electric field gradients obtained from this analysis can be used to gauge relative populations of the atomic p orbitals for the bromine atom and proved to be quite useful in assigning the *b* and *c* inertial axes.

Experimental Section

Various syntheses for allyltricarbyliron bromide can be found in the literature, including a photochemical reaction,⁶ a displacement reaction,⁷ and a ligand exchange.⁸ The first method, in which the allyl bromide is split into allyl and bromide radicals, is a photoinduced radical attack on iron pentacarbonyl, resulting in the displacement of two carbonyl ligands with the allyl group and bromine atom. The second method is less efficient in the respect that each 1 mol of allyl bromide reacts with 1 equiv of Fe₂(CO)₉ to produce the desired product and 1 equiv each of iron pentacarbonyl and free carbon monoxide. The third method requires preparation of a similar iodo species prior to ligand exchange with (Et)₄NBr. The second method, described originally by Murdoch and Weiss,⁷ was chosen because of the simplicity of the system, rapid reaction time, and ability to efficiently separate the product from iron pentacarbonyl and unreacted Fe₂(CO)₉ through sublimation. The proton NMR spectrum in CDCl₃ was identical to that described by Nesmeyonov,⁴ showing both anti and syn forms in a ~4:1 ratio.

The solid sample was manipulated under a dry N₂(g) atmosphere and loaded into a glass sample chamber. The sample chamber, attached to a General Valve Series 9 pulsed valve with a 2 mm orifice, was held at 50 °C with 1 atm neon during collection of the rotational spectra. Over 400 transitions with *J'* ← *J* from 3 ← 2 to 5 ← 4 for the two isomers and two bromine isotopomers (each) were measured in the 5–9 GHz range. The measured transitions with quantum number assignments are listed in Tables 1–4. The main isotopomer (⁷⁹Br or ⁸¹Br, ⁵⁶Fe) transitions for each isomer are listed separately in Tables 1 (anti) and 2 (syn). A few transitions believed to be due to the ⁵⁴Fe isotopomers of the anti isomer were also identified in the spectrum and are listed in Tables 3 (⁷⁹Br) and 4 (⁸¹Br). The columns labeled \bar{F}^* ($\bar{F}^* = F + 1/2$) indicate the total angular momentum \bar{F} ($\bar{F} = \bar{I}_{\text{Br}} + \bar{J}$). Although the intensity data in the experiment is subject to variations in cavity modes and input power, the intensities of transitions for *syn*-allyltricarbyliron bromide were consistently 10 times weaker than the intensities for corresponding transitions for the anti form. Since the dipole moments of the two isomers should be very similar, it is reasonable to assume that the anti form is the predominant component of the gas-phase, pulsed-beam sample.

Data Analysis

Rotational transitions expected for an “*a*” dipole near-prolate symmetric top with quadrupole coupling were measured and assigned for both isomers. Transitions that could be assigned to either a “*b*” or “*c*” type dipole spectrum were also measured for the two isomers. Patterns for the *b* or *c* type transitions were more easily identified due to stronger signal intensities and relatively larger separations between quadrupole components. The *a* axis is very nearly aligned with the Fe–Br bond direction. The frequency splittings between different *K*₀ components of the *b* or *c* type transitions were similar in magnitude to the splittings between different R-branch (*J'* ← *J*) principal rotational transitions. The observed quadrupole splittings are on the order of 50 MHz. Therefore, overlap between asymmetry and quadrupole splittings in the *b* (or *c*) type transitions was not generally observed in the low-frequency region of the spectrum. For these transitions, however, overlapping spectral patterns due to two isotopes of bromine, which are approximately equal in concentration, were observed. The quadrupole moment ratio was used to identify these ⁷⁹Br and ⁸¹Br splitting patterns in the spectra. The *a* type transitions are well separated both for the different isotopomers of bromine and principal rotational transitions. However, many of the transitions had severely overlapping quadrupole and asymmetry patterns. It was not until reasonable values for the diagonal quadrupole tensor elements χ_{aa} and χ_{bb} were determined from preliminary assignment of the *c* (*b* for the syn isomer) dipole transitions that a satisfactory assignment for the *a* dipole quadrupole splitting pattern could be made. Successful assignment of a majority of the measured transitions was made only after including off-diagonal quadrupole terms using Herb Pickett's program SPFIT.⁹

Once a suitable number of transitions (> 50) was assigned, the entire quadrupole coupling tensor could be determined with reasonable accuracy. The molecules each contain a plane of symmetry. This is the *ac* plane for the anti isomer and *ab* plane for the syn isomer. The determination of which axis system is appropriate to use for each isomer was made after successful assignment of the transitions and is discussed later. The presence of the symmetry plane requires that the appropriate values (χ_{ab} , χ_{bc} or χ_{ac} , χ_{bc} , respectively) of the quadrupole coupling tensor are zero. The remaining off-diagonal component is only very weakly dependent on the measured transition frequencies, particularly for low *F* transitions and the weak $\Delta F = 0$ transitions.

Due to the near symmetric top character of these molecules, the five quartic distortion constants are very difficult to determine from the measured spectra. The *D*_{*K*} constant was highly correlated with the *A* rotational constant and the δ_J and δ_K values are correlated with $(B - C)/2$. The data set for the main isotopomers of the anti conformation was large enough to determine the entire set of quartic distortion constants to reasonable accuracy. Attempts to vary all of the quartic distortion constants for the syn conformation resulted in poorly determined values of *D*_{*J*}, δ_J , and *D*_{*K*}, and therefore, the only distortion constants varied were *D*_{*J*} and *D*_{*JK*}. The measured transitions are all for low values of *J* and *K*, so errors in the rotational constants due to correlation with undetermined distortion constants should remain minimal.

The spectral fits included 168 (144 measured, with 24 pairs of unresolved *K* components) transitions for *anti*-C₃H₅Fe(CO)₃⁷⁹Br, 129 (119) transitions for *anti*-C₃H₅Fe(CO)₃⁸¹Br, 104

(4) Nesmeyonov, A. N.; Ustynyuk, Y. A.; Kritskaya, I. I.; Shchembelov, G. A. *J. Organomet. Chem.* **1968**, *14*, 395.

(5) Hirota, E.; Yamada, C. *J. Chem. Phys.* **1992**, *97*, 2963.

(6) Heck, R. F.; Boss, C. R. *J. Am. Chem. Soc.* **1964**, *86*, 2580.

(7) Murdoch, H. D.; Weiss, E. *Helv. Chim. Acta* **1962**, *45*, 1927.

(8) Nesmeyonov, A. N.; Kritskaya, I. I. *J. Organomet. Chem.* **1968**, *14*, 387.

(9) Pickett, H. M. *J. Mol. Spectrosc.* **1991**, *148*, 371 (see also <http://spec.jpl.nasa.gov/>).

Table 1. Measured Transition Frequencies for ^{79}Br , ^{81}Br anti- $\text{C}_3\text{H}_5\text{Fe}(\text{CO})_3\text{Br}^a$

anti ^{79}Br	anti ^{81}Br	$J'_{K_p',K_o'}$	$F^{*'}_1$	J_{K_p,K_o}	F^*_1	anti ^{79}Br	anti ^{81}Br	J_{K_p,K_o}	F^*_1	$J'_{K_p',K_o'}$	$F^{*'}_1$	J_{K_p,K_o}	F^*_1
5092.6134(42)	5102.6685(29)	3 ₃₀	4	2 ₂₀	4	6959.8800(30)				6 ₄₂	7	5 ₄₁	7
5092.6134(42)	5102.6685(29)	3 ₃₁	4	2 ₂₁	4	6962.9102(06)				6 ₁₆	6	5 ₁₅	6
5164.8432(05)	5163.0992(16)	3 ₃₀	3	2 ₂₀	2	6963.0503(21)	6907.6211(15)			6 ₅₁	8	5 ₅₀	7
5164.8432(05)	5163.0992(16)	3 ₃₁	3	2 ₂₁	2	6964.5581(45)				6 ₃₄	5	5 ₃₃	5
5175.5722(16)	5172.1005(28)	3 ₃₀	4	2 ₂₀	3	6964.6051(23)				6 ₀₆	6	5 ₀₅	6
5175.5722(16)	5172.1005(28)	3 ₃₁	4	2 ₂₁	3	6970.6947(22)				6 ₄₂	8	5 ₄₁	7
5185.1067(19)	5180.1263(32)	3 ₃₀	2	2 ₂₀	1	6971.3951(35)				6 ₃₄	5	5 ₃₃	4
5185.1067(19)		3 ₃₁	2	2 ₂₁	1	6971.3951(35)				6 ₃₃	5	5 ₃₂	4
5196.5036(13)	5189.5881(14)	3 ₃₀	5	2 ₂₀	4	6976.5429(35)	6918.8742(26)			6 ₃₄	8	5 ₃₃	7
5196.5036(13)	5189.5881(14)	3 ₃₁	5	2 ₂₁	4	6976.5429(35)	6918.8742(26)			6 ₃₃	8	5 ₃₂	7
	5212.1178(25)	3 ₃₀	3	2 ₂₀	3	6978.3515(10)	6919.6769(24)			6 ₁₆	8	5 ₁₅	7
5271.0041(10)	5251.6025(37)	3 ₃₀	2	2 ₂₀	2	6980.2869(76)	6922.0511(63)			6 ₂₅	5	5 ₂₄	4
5271.0041(10)	5251.6025(37)	3 ₃₁	2	2 ₂₁	2	6980.4710(55)				6 ₂₄	5	5 ₂₃	4
5740.6968(13)		5 ₀₅	4	4 ₀₄	4	6980.6093(16)	6922.2724(56)			6 ₂₅	8	5 ₂₄	7
5748.7086(25)	5808.6866(42)	5 ₄₂	6	4 ₄₁	6	6980.6531(28)	6921.6124(32)			6 ₁₆	7	5 ₁₅	6
	5749.3670(12)	5 ₃₂	4	4 ₃₁	3	6980.7921(20)	6922.4436(44)			6 ₂₄	8	5 ₂₃	7
	5751.4533(13)	5 ₁₅	5	4 ₁₄	5	6981.0320(21)	6921.9424(47)			6 ₁₆	5	5 ₁₅	4
5771.6567(99)		5 ₄₂	4	4 ₄₁	3	6983.4668(12)	6923.9676(10)			6 ₁₆	6	5 ₁₅	5
	5771.7607(23)	5 ₁₅	5	4 ₁₄	4	6983.6630(52)	6924.8119(13)			6 ₀₆	7	5 ₀₅	6
	5775.4163(12)	5 ₃₂	4	4 ₃₁	4	6983.6969(90)	6924.8490(32)			6 ₀₆	8	5 ₀₅	7
	5736.3872(30)	5 ₂₄	4	4 ₂₃	4	6987.3491(39)	6927.9241(88)			6 ₀₆	6	5 ₀₅	5
5778.8983(41)	5736.4780(32)	5 ₂₃	4	4 ₂₂	4	6987.4203(20)	6927.9623(23)			6 ₀₆	5	5 ₀₅	4
	5788.9228(14)	5 ₃₂	5	4 ₃₁	5	6987.7175(13)	6928.9243(16)			6 ₁₅	8	5 ₁₄	7
	5791.5055(12)	5 ₃₂	6	4 ₃₁	5	6989.9419(14)	6930.0999(27)			6 ₂₅	7	5 ₂₄	6
5794.1425(05)		5 ₃₃	4	4 ₃₂	3	6990.0146(73)	6930.8604(42)			6 ₁₅	7	5 ₁₄	6
5794.1425(05)		5 ₃₂	4	4 ₃₁	3	6990.1504(99)	6930.2727(99)			6 ₂₅	6	5 ₂₄	5
5796.3699(28)	5751.0589(08)	5 ₀₅	5	4 ₀₄	5	6990.3562(99)	6930.4452(29)			6 ₂₄	6	5 ₂₃	5
5797.6327(05)	5752.2424(14)	5 ₄₂	7	4 ₄₁	6	6990.4201(49)	6931.2085(41)			6 ₁₅	5	5 ₁₄	4
5805.1291(28)		5 ₁₄	5	4 ₁₃	5	6992.8591(24)	6933.2393(19)			6 ₁₅	6	5 ₁₄	5
5807.2605(09)	5760.2669(09)	5 ₃₃	7	4 ₃₂	6	6993.4456(30)	6932.9907(41)			6 ₃₄	6	5 ₃₃	5
5807.2605(09)	5760.2669(09)	5 ₃₂	7	4 ₃₁	6	6993.4456(30)	6932.9907(41)			6 ₃₃	6	5 ₃₂	5
5810.9254(14)	5763.4097(39)	5 ₂₄	4	4 ₂₃	3	6997.7430(32)				6 ₃₄	7	5 ₃₃	6
5811.0257(26)	5763.5050(35)	5 ₂₃	4	4 ₂₂	3	6997.7906(34)	6936.5998(13)			6 ₄₂	6	5 ₄₁	5
5813.9636(58)	5765.8650(19)	5 ₂₄	7	4 ₂₃	6	7003.1124(18)				6 ₅₁	6	5 ₅₀	5
5814.0190(14)	5765.3316(21)	5 ₁₅	7	4 ₁₄	6	7007.3140(20)	6944.4739(15)			6 ₃₄	7	5 ₃₃	7
5814.0624(26)	5765.9600(16)	5 ₂₃	7	4 ₂₂	6	7008.8007(16)	6945.8561(12)			6 ₄₂	7	5 ₄₁	6
5816.0720(46)	5767.6942(19)	5 ₂₄	5	4 ₂₃	5	7010.6530(42)	6947.5299(39)			6 ₄₂	6	5 ₄₁	6
5816.1786(45)		5 ₂₃	5	4 ₂₂	5	7014.2279(07)	7011.1390(16)			4 ₄₀	4	3 ₃₀	3
5816.8343(14)		5 ₃₃	6	4 ₃₂	6	7021.7064(20)	7017.4237(08)			4 ₄₀	5	3 ₃₀	4
5817.4016(11)	5768.1933(07)	5 ₁₅	4	4 ₁₄	3	7023.4321(35)	6958.0055(28)			6 ₅₁	7	5 ₅₀	6
5818.0422(09)	5768.7116(05)	5 ₁₅	6	4 ₁₄	5	7026.3590(25)	7021.3333(12)			4 ₄₀	3	3 ₃₀	2
5819.1098(16)	5770.1703(23)	5 ₀₅	6	4 ₀₄	5	7026.3590(25)	7021.3333(12)			4 ₄₁	3	3 ₃₁	2
5819.1577(18)	5770.2107(12)	5 ₀₅	7	4 ₀₄	6	7034.3868(45)	7028.0043(13)			4 ₄₀	6	3 ₃₀	5
5821.8235(23)	5773.0362(13)	5 ₁₄	7	4 ₁₃	6	7040.9155(99)				6 ₂₅	7	5 ₂₄	7
5824.6187(08)	5774.8096(23)	5 ₀₅	5	4 ₀₄	4	7041.1127(25)				6 ₂₄	7	5 ₂₃	7
5824.7677(11)	5774.9133(48)	5 ₀₅	4	4 ₀₄	3	7056.0774(16)	6984.5895(12)			6 ₁₆	7	5 ₁₅	7
5825.2407(31)	5775.9320(20)	5 ₁₄	4	4 ₁₃	3	7061.9356(18)	7051.1548(10)			4 ₄₀	4	3 ₃₀	4
5825.8494(10)	5776.4220(24)	5 ₁₄	6	4 ₁₃	5	7065.9070(20)				6 ₁₅	7	5 ₁₄	7
5828.2786(25)	5777.8319(33)	5 ₂₄	5	4 ₂₃	4	7494.1921(32)				5 ₃₂	5	4 ₂₂	5
5828.3833(36)	5777.9297(36)	5 ₂₃	5	4 ₂₂	4	7497.4267(54)	7475.3667(48)			5 ₃₂	6	4 ₂₂	5
5829.5315(25)	5779.5050(25)	5 ₁₄	5	4 ₁₃	4	7497.5005(34)	7475.4316(26)			5 ₃₃	6	4 ₂₃	5
5830.3043(40)	5779.5749(45)	5 ₂₄	6	4 ₂₃	5		7504.1499(65)			5 ₃₂	6	4 ₂₂	6
5830.4127(28)	5779.6781(22)	5 ₂₃	6	4 ₂₂	5	7506.4045(17)	7482.9186(88)			5 ₃₂	5	4 ₂₂	4
5832.5073(33)	5781.3362(13)	5 ₃₃	5	4 ₃₂	4	7506.4643(37)	7482.9839(26)			5 ₃₃	5	4 ₂₃	4
5832.5073(33)	5781.3362(13)	5 ₃₂	5	4 ₃₁	4	7522.4837(42)	7496.3127(37)			5 ₃₂	7	4 ₂₂	6
	5836.4198(23)	5 ₁₄	6	4 ₁₃	6	7522.5441(46)	7496.3695(32)			5 ₃₃	7	4 ₂₃	6
	5785.8785(19)	5 ₄₂	5	4 ₄₁	4	7531.6909(56)	7504.0227(43)			5 ₃₂	4	4 ₂₂	3
5837.9168(12)		5 ₃₂	6	4 ₃₁	5	7531.7461(63)	7504.0982(56)			5 ₃₃	4	4 ₂₃	3
5844.5857(03)		4 ₃₁	5	3 ₂₁	4		8061.8301(44)			7 ₁₇	7	6 ₁₆	7
6330.6137(36)	6318.8559(40)	4 ₃₂	5	3 ₂₂	4		8076.7280(48)			7 ₁₇	7	6 ₁₆	6
6330.6596(49)	6318.8852(68)	4 ₃₁	4	3 ₂₁	3		8091.3632(15)			7 ₅₃	7	6 ₅₂	6
6340.6854(25)	6327.3009(59)	4 ₃₂	4	3 ₂₂	3		8095.3382(28)			7 ₆₂	7	6 ₆₁	6
6340.7228(13)		4 ₃₁	6	3 ₂₁	5		8108.3985(26)			7 ₆₂	8	6 ₆₁	7
6369.6751(72)	6351.5662(46)	4 ₃₁	3	3 ₂₁	2	8113.9303(16)				7 ₆₂	6	6 ₆₁	5
	6906.7108(44)	6 ₁₆	6	5 ₁₅	6	8124.9274(24)	8060.0219(17)			7 ₅₃	6	6 ₅₂	5
6917.8176(48)		4 ₄₀	5	3 ₃₀	5	8128.5544(26)	8063.0686(23)			7 ₆₂	9	6 ₆₁	8
	6918.3737(82)	6 ₂₅	6	5 ₂₄	6	8131.6061(17)				7 ₀₇	7	6 ₀₆	7
	6918.5554(30)	6 ₂₄	6	5 ₂₃	6	8134.7236(03)				7 ₅₃	9	6 ₅₂	8
	6936.6367(29)	6 ₃₃	7	5 ₃₂	6	8138.9702(29)				7 ₁₆	7	6 ₁₅	7
	6941.0809(23)	6 ₅₂	6	5 ₅₁	5	8139.7006(14)				7 ₄₄	9	6 ₄₃	8
6943.9547(11)		6 ₅₁	5	5 ₅₀	4	8141.4731(23)				7 ₃₅	6	6 ₃₄	5
6959.1670(09)	6947.6281(45)	6 ₄₂	5	5 ₄₁	5	8141.4731(23)				7 ₃₄	6	6 ₃₃	5

Table 1 (Continued)

anti ⁷⁹ Br	anti ⁸¹ Br	$J'_{K_p, K_o'}$	F^{*a}	J_{K_p, K_o}	F^*	anti ⁷⁹ Br	anti ⁸¹ Br	$J'_{K_p, K_o'}$	F^{*a}	J_{K_p, K_o}	F^*
8142.2845(14)		7 ₁₇	9	6 ₁₆	8	8154.6526(17)		7 ₁₆	8	6 ₁₅	7
8143.5427(44)		7 ₃₅	9	6 ₃₄	8	8155.2613(21)		7 ₃₅	7	6 ₃₄	6
8143.5427(44)		7 ₃₄	9	6 ₃₃	8	8155.3371(17)		7 ₁₆	6	6 ₁₅	5
8143.7244(34)		7 ₁₇	8	6 ₁₆	7	8156.7639(24)		7 ₃₄	8	6 ₃₃	7
8144.3947(16)		7 ₁₇	6	6 ₁₆	5	8156.7639(24)		7 ₃₅	8	6 ₃₄	7
8146.1675(34)		7 ₂₆	9	6 ₂₅	8	8156.8475(43)		7 ₁₆	7	6 ₁₅	6
8146.4580(48)		7 ₂₅	9	6 ₂₄	8	8158.4512(21)		7 ₄₄	7	6 ₄₃	6
8146.6904(32)		7 ₂₆	6	6 ₂₅	5	8162.4551(32)		7 ₅₃	7	6 ₅₂	6
8146.9744(70)		7 ₂₅	6	6 ₂₄	5	8163.3790(20)	8092.1811(32)	7 ₄₄	8	6 ₄₃	7
8147.7388(64)		7 ₃₅	7	6 ₃₄	7	8172.0489(19)	8099.4012(10)	7 ₅₃	8	6 ₅₂	7
8147.7388(64)		7 ₃₄	7	6 ₃₃	7	8178.1948(24)	8165.3642(18)	5 ₄₁	6	4 ₃₁	5
8148.0227(25)		7 ₀₇	8	6 ₀₆	7	8178.1948(24)	8165.3642(18)	5 ₄₂	6	4 ₃₂	5
8148.0639(23)		7 ₀₇	9	6 ₀₆	8	8182.2089(24)	8168.7028(19)	5 ₄₁	5	4 ₃₁	4
	8149.3193(30)	7 ₀₇	8	6 ₀₆	8	8182.2089(24)	8168.7028(19)	5 ₄₂	5	4 ₃₂	4
8150.4399(58)		5 ₄₁	6	4 ₃₁	6	8191.0603(20)	8176.2885(35)	5 ₄₁	5	4 ₃₁	5
8150.4399(58)		5 ₄₂	6	4 ₃₂	6	8191.0603(20)	8176.2885(35)	5 ₄₂	5	4 ₃₂	5
8150.6685(15)		7 ₀₇	7	6 ₀₆	6	8199.3641(07)	8183.0225(26)	5 ₄₁	7	4 ₃₁	6
8150.7201(52)		7 ₀₇	6	6 ₀₆	5	8199.3641(07)	8183.0225(26)	5 ₄₂	7	4 ₃₂	6
	8151.0127(35)	7 ₁₆	8	6 ₁₅	8	8202.7228(13)	8185.8986(29)	5 ₄₁	4	4 ₃₁	3
8152.0045(26)		7 ₂₆	8	6 ₂₅	7	8202.7228(13)	8185.8986(29)	5 ₄₂	4	4 ₃₂	3
8152.3037(09)		7 ₂₅	8	6 ₂₄	7		8211.9472(19)	5 ₄₂	4	4 ₃₂	4
8152.8348(34)		7 ₂₆	7	6 ₂₅	6		8211.9472(19)	5 ₄₁	4	4 ₃₁	4
8153.1335(42)		7 ₂₅	7	6 ₂₄	6	8212.3044(14)	8132.9843(15)	7 ₂₆	8	6 ₂₅	8
8153.2100(29)		7 ₁₆	9	6 ₁₅	8	8212.6211(25)	8133.2835(18)	7 ₂₅	8	6 ₂₄	8

^a $F^* = F + 1/2$. All frequencies are in MHz with listed 1σ uncertainties in the last significant digits.

(80) transitions for *syn*-C₃H₅Fe(CO)₃⁷⁹Br, and 74 (60) transitions for *syn*-C₃H₅Fe(CO)₃⁸¹Br. For the limited data sets of *anti*-C₃H₅⁵⁴Fe(CO)₃⁷⁹Br (and ⁸¹Br) the distortion constants and a few quadrupole elements were each fixed at the values determined for the main isotopomer. The molecular parameters determined from the spectral fitting analyses are given in Tables 5 and 6.

DFT Calculations

Calculations were performed on an SGI Origin 2000 computer using the algorithms of Gaussian94 revision E.2.¹⁰ The density functional methods of Becke,^{11a-c} Perdew, and Wang^{11d} (BPW91) were applied for a geometry optimization of the structure of *anti*- and *syn*-allyltricarbyliron bromide. The 6-311G basis sets were used for all atoms. The optimized geometries were verified to be true minima on the multidimensional potential energy surface through frequency calculations that indicated all real positive force constants.

The crystal structure,³ with an artificially inserted central hydrogen atom, was used as the input initial geometry for the DFT geometry optimization of the *anti* isomer. The calculated atomic coordinates for the *anti* isomer are listed in Table 7. The structure is shown in Figure 1a. For the initial structure of the *syn* isomer, the Fe(CO)₃Br base of the *anti* conformation was used and the allyl group coordinates were reflected through the plane containing the equatorial carbonyls. The optimized structure was quite different from this first guess structure but nonetheless had the correct, opposite orientation of the allyl group relative to the *anti* conformer. The geometry for the *syn* isomer is shown alongside the *anti* form in Figure 1b, and the atomic coordinates are listed in Table 8. Calculations indicate that the *anti* isomer lies 609 cm⁻¹ (1.7 kcal mol⁻¹) lower in energy than the *syn* form.

Structural Refinement of the Anti Conformation

With four isotopomers identified in the spectrum for the *anti* isomer, it is possible to do a partial structural determination using selected adjustable parameters in a fit to the 12 experimentally determined moments of inertia. Using the Cartesian coordinate fitting program written by Schwendeman et al.¹² the ligand geometry has been refined. Since ¹³C-substituted spectra were not available, no attempts to independently fit the entire set of coordinates were made. Instead, selected constraints were used that allowed the ligand positions to change with respect to the iron atom. Generally, the internal coordinates of the ligands were fixed. The following coordinates were varied: (1) $a_o(\text{Br})$; (2) $c_o(\text{Br})$; (3) $a_o(\text{Fe})$; (4) $c_o(\text{Fe})$; (5) $a_o(\text{C1,C2,C3,H1,H2,H3,H4,H5})$; (6) $b_o(\text{C1,C3,H2,H3,H4,H5})$; (7) $c_o(\text{C1,C2,C3,H1,H2,H3,H4,H5})$; (8) $a_o(\text{C4,C6,O1,O3})$; (9) $b_o(\text{C4,C6,O1,O3})$; (10) $c_o(\text{C4,C6,O1,O3})$; (11) $a_o(\text{C5,O2})$; (12) $c_o(\text{C5,O2})$. The notation here lists the parameter number, followed by the coordinate (a_o , b_o , or c_o) with the atom(s) in parentheses. The atom numbering scheme is shown in Figure 2. A list of multiple atoms with a single parameter indicates that these "constrained" atomic coordinates were adjusted simultaneously using this single variable. The b coordinates for atoms in the symmetry plane are absent from the list since these were assumed to be zero. Fitting Cartesian coordinates introduces redundancy in the definition of parameters (e.g. the Fe-Br bond length requires four parameters!), and it appears that there are 12 variables to fit 12 parameters. However, the number of variables is reduced by satisfying the first moment conditions, and this condition is included in the analyses for the a and c centers of mass. This effectively reduces the number of variable parameters to 10.

Linear combinations of the parameters listed above can be used to describe the changes in the initial structure. The variable parameters used in the structure fit allow the following: (i)

(10) Frisch, M. J.; Trucks, G. W.; Schlegel, H. B.; Gill, P. M. W.; Johnson, B. G.; Robb, M. A.; Cheeseman, J. R.; Keith, T.; Petersson, G. A.; Montgomery, A. J.; Raghavachari, K.; Al-Laham, M. A.; Zakrzewski, V. G.; Ortiz, J. V.; Foresman, J. B.; Peng, C. Y.; Ayala, P. Y.; Chen, W.; Wong, M. W.; Andres, J. L.; Replogle, E. S.; Gomperts, R.; Martin, R. L.; Fox, D. J.; Binkley, J. S.; Defrees, D. J.; Baker, J.; Stewart, J. P.; Head-Gordon, M.; Gonzalez, C.; Pople, J. A. *Gaussian 94, Revision B.3*; Gaussian, Inc.: Pittsburgh, PA, 1995.

(11) (a) Becke, A. D. *Phys. Rev.* **1988**, A38, 3098. (b) *ACS Symp. Ser.* **1989**, No. 394, 165. (c) *Int. J. Quantum Chem. Symp.* **1989**, No. 23, 599. (d) Perdew, J. P.; Wang, Y. *Phys. Rev.* **1992**, B45, 13, 244.

(12) Schwendeman, R. H. In *Critical Evaluation of Chemical and Physical Structural Information*; Lide, D. R., Paul, M. A., Eds.; National Academy of Sciences: Washington, DC, 1974; p 74.

Table 2. Measured Transition Frequencies for ⁷⁹Br, ⁸¹Br *syn*-C₃H₅Fe(CO)₃Br^a

syn ⁷⁹ Br	syn ⁸¹ Br	<i>J'</i> _{K_p,K_o'}	<i>F</i> *'	<i>J</i> _{K_p,K_o}	<i>F</i> *	syn ⁷⁹ Br	syn ⁸¹ Br	<i>J'</i> _{K_p,K_o'}	<i>F</i> *'	<i>J</i> _{K_p,K_o}	<i>F</i> *
5158.2381(36)	5156.5608(37)	3 ₃₁	3	2 ₂₀	2	6989.4309(56)		6 ₂₄	7	5 ₂₃	6
5158.2381(36)	5156.5608(37)	3 ₃₀	3	2 ₂₁	2	6989.6696(87)		6 ₂₄	6	5 ₂₃	5
5169.4138(36)	5165.9677(99)	3 ₃₁	4	2 ₂₀	3	6996.4435(23)	6937.0510(02)	6 ₁₅	7	5 ₁₄	6
5169.4595(48)		3 ₃₁	4	2 ₂₁	3	6996.9483(31)	6937.4852(03)	6 ₁₅	5	5 ₁₄	4
	5184.2262(56)	3 ₃₁	5	2 ₂₀	4	7005.7490(23)		4 ₄₁	4	3 ₃₀	3
	5184.2776(45)	3 ₃₀	5	2 ₂₁	4	7005.7490(23)		4 ₄₀	4	3 ₃₁	3
	5746.5840(18)	5 ₃₃	4	4 ₃₂	3	7007.8141(12)	6944.5820(17)	6 ₄₃	7	5 ₄₂	6
	5757.9847(13)	5 ₃₃	7	4 ₃₂	6	7007.8141(12)	6944.5820(17)	6 ₄₂	7	5 ₄₁	6
	5757.9847(13)	5 ₃₂	7	4 ₃₁	6	7013.5518(16)	7009.2584(08)	4 ₄₁	5	3 ₃₀	4
	5759.3448(07)	5 ₁₅	6	4 ₁₄	5	7013.5518(16)	7009.2584(08)	4 ₄₀	5	3 ₃₁	4
5775.0613(39)	5761.0341(11)	5 ₂₄	4	4 ₂₃	4	7018.4188(38)	7013.3376(60)	4 ₄₁	3	3 ₃₀	2
	5780.0061(16)	5 ₃₂	5	4 ₃₁	4	7018.4188(38)	7013.3376(60)	4 ₄₀	3	3 ₃₁	2
	5780.0061(16)	5 ₃₃	5	4 ₃₂	4	7023.0965(22)		6 ₅₁	7	5 ₅₀	6
5791.2497(30)	5746.5840(18)	5 ₃₂	4	4 ₃₁	3	7023.0965(22)		6 ₅₂	7	5 ₅₁	6
5791.2497(30)	5746.5840(18)	5 ₃₂	4	4 ₃₁	3	7026.8032(12)	7020.3108(13)	4 ₄₁	6	3 ₃₀	5
5794.8603(23)	5749.5482(64)	5 ₄₂	7	4 ₄₁	6	7026.8032(12)	7020.3108(13)	4 ₄₀	6	3 ₃₁	5
5804.4707(30)	5755.8326(10)	5 ₁₅	7	4 ₁₄	6		7044.4782(23)	4 ₄₁	4	3 ₃₀	4
5804.9775(21)		5 ₃₃	7	4 ₃₂	6		7044.4782(23)	4 ₄₀	4	3 ₃₁	4
5804.9775(21)		5 ₃₂	7	4 ₃₁	6	7046.6725(36)		6 ₁₆	7	5 ₁₅	7
5807.8963(09)		5 ₁₅	4	4 ₁₄	3		7467.8588(14)	5 ₃₃	6	4 ₂₂	5
5809.4290(13)		5 ₂₃	4	4 ₂₂	3		7468.5953(09)	5 ₃₂	6	4 ₂₃	5
5811.7501(18)	5763.6155(06)	5 ₂₄	7	4 ₂₃	6	7499.2406(24)	7475.7678(53)	5 ₃₃	5	4 ₂₂	4
5812.3696(33)	5762.4616(36)	5 ₁₅	5	4 ₁₄	4	7499.9867(50)	7476.4657(20)	5 ₃₂	5	4 ₂₃	4
5812.6370(08)	5764.4675(28)	5 ₂₃	7	4 ₂₂	6	7516.0888(51)	7489.8012(44)	5 ₃₃	7	4 ₂₂	6
5816.3736(27)	5767.4081(20)	5 ₀₅	6	4 ₀₄	5	7516.7479(99)	7490.4394(48)	5 ₃₂	7	4 ₂₃	6
5816.4826(14)	5767.4886(18)	5 ₀₅	7	4 ₀₄	6		7497.8770(57)	5 ₃₃	4	4 ₂₂	3
5822.3498(15)		5 ₀₅	4	4 ₀₄	3	7526.3561(18)	7498.4909(30)	5 ₃₂	4	4 ₂₃	3
5826.7034(31)		5 ₂₄	5	4 ₂₃	5		8062.0387(65)	7 ₁₇	5	6 ₁₆	5
5827.1388(17)	5778.1762(44)	5 ₁₄	7	4 ₁₃	6		8097.7172(23)	7 ₅₂	8	6 ₅₁	7
5827.6484(13)	5777.0093(25)	5 ₂₃	5	4 ₂₂	4	8109.9461(58)		7 ₆₂	6	6 ₆₁	5
5828.7995(07)		5 ₂₄	6	4 ₂₃	5	8125.1834(55)		7 ₆₂	9	6 ₆₁	8
	5829.8516(56)	5 ₄₂	4	4 ₄₁	4	8126.0847(49)		7 ₀₇	7	6 ₀₆	7
5830.7957(11)		5 ₁₄	4	4 ₁₃	3	8128.7344(47)	8060.2101(40)	7 ₁₇	9	6 ₁₆	8
5831.3224(17)	5781.6904(15)	5 ₁₄	6	4 ₁₃	5	8130.2194(19)	8061.4577(19)	7 ₁₇	8	6 ₁₆	7
5831.3663(15)		5 ₃₃	5	4 ₃₂	4	8130.8951(31)		7 ₁₇	6	6 ₁₆	5
5831.3663(15)		5 ₃₂	5	4 ₃₁	4	8131.1161(28)		7 ₄₄	6	6 ₄₃	5
5835.2665(14)	5784.9918(15)	5 ₁₄	5	4 ₁₃	4	8131.1161(28)		7 ₄₃	6	6 ₄₂	5
5836.9548(29)	5784.6981(23)	5 ₄₂	5	4 ₄₁	4	8131.6602(43)		7 ₅₂	9	6 ₅₁	8
5843.9607(06)	5790.6122(12)	5 ₃₃	6	4 ₃₂	5	8131.6602(43)		7 ₅₃	9	6 ₅₂	8
5843.9607(06)	5790.6122(12)	5 ₃₂	6	4 ₃₁	5	8132.4552(27)		7 ₁₇	7	6 ₁₆	6
	6912.0302(28)	6 ₃₄	5	5 ₃₃	4	8136.9301(21)		7 ₄₃	9	6 ₄₂	8
	6912.0302(28)	6 ₃₃	5	5 ₃₂	4	8136.9301(21)		7 ₄₃	9	6 ₄₂	8
	6912.6395(22)	6 ₁₆	6	5 ₁₅	5	8145.6856(66)		7 ₂₅	9	6 ₂₄	8
	6916.4757(48)	6 ₃₃	8	5 ₃₂	7	8145.9058(27)		7 ₀₇	7	6 ₀₆	6
	6918.5069(73)	4 ₄₁	5	3 ₃₀	5	8146.0425(51)		7 ₀₇	6	6 ₀₆	5
	6918.5069(73)	4 ₄₀	5	3 ₃₁	5	8149.2605(36)		7 ₂₆	8	6 ₂₅	7
	6920.9026(24)	6 ₂₄	5	5 ₂₃	4	8150.1299(36)		7 ₂₆	7	6 ₂₅	6
	6921.1859(15)	6 ₀₆	8	5 ₀₅	7	8152.7255(36)		7 ₂₅	7	6 ₂₄	6
	6924.3334(34)	6 ₀₆	5	5 ₀₅	5	8154.9036(22)		7 ₃₄	8	6 ₃₃	7
	6924.4526(36)	6 ₀₆	5	5 ₀₅	4	8156.5241(37)		7 ₄₄	7	6 ₄₃	6
	6934.9359(22)	6 ₄₂	6	5 ₄₁	5	8156.5241(37)		7 ₄₃	7	6 ₄₂	6
	6935.0155(38)	6 ₃₄	7	5 ₃₃	6	8160.4985(54)	8091.5092(44)	7 ₁₆	9	6 ₁₅	8
	6935.0503(24)	6 ₁₅	8	5 ₁₄	7	8160.6502(32)		7 ₅₃	7	6 ₅₂	6
	6939.5922(46)	6 ₅₂	6	5 ₅₁	5	8161.6595(19)	8090.2224(19)	7 ₄₄	8	6 ₄₃	7
6940.0764(39)		6 ₅₁	5	5 ₅₀	4	8161.6595(19)	8090.2224(19)	7 ₄₃	8	6 ₄₂	7
6955.9602(21)		6 ₄₃	5	5 ₄₂	4	8161.9783(22)	8092.7520(19)	7 ₁₆	8	6 ₁₅	7
6955.9602(21)		6 ₄₂	5	5 ₄₁	4	8162.7625(65)		7 ₁₆	6	6 ₁₅	5
	6957.2624(21)	6 ₅₂	7	5 ₅₁	6	8164.3242(47)	8094.7127(27)	7 ₁₆	7	6 ₁₅	6
6959.9796(61)		6 ₅₁	8	5 ₅₀	7	8169.3254(30)		5 ₄₂	6	4 ₃₁	5
6959.9796(61)		6 ₅₂	8	5 ₅₁	7	8169.3254(30)		5 ₄₁	6	4 ₃₂	5
6966.8367(25)	6908.2229(21)	6 ₁₆	8	5 ₁₅	7	8170.6659(11)		7 ₅₃	8	6 ₅₂	7
6968.0096(24)		6 ₄₃	8	5 ₄₂	7		8097.7172(23)	7 ₅₂	8	6 ₅₁	7
6968.0096(24)		6 ₄₂	8	5 ₄₁	7	8173.5342(06)		5 ₄₂	5	4 ₃₁	4
6969.2185(17)	6910.2252(27)	6 ₁₆	7	5 ₁₅	6	8173.5342(06)		5 ₄₁	5	4 ₃₂	4
6969.5721(22)		6 ₁₆	5	5 ₁₅	4	8191.4522(22)		5 ₄₂	7	4 ₃₁	6
6974.2024(35)		6 ₃₄	8	5 ₃₃	7	8191.4522(22)		5 ₄₁	7	4 ₃₂	6
6974.2024(35)		6 ₃₄	8	5 ₃₃	7	8194.9431(35)		5 ₄₂	4	4 ₃₁	3
6983.8173(28)	6924.3334(34)	6 ₀₆	6	5 ₀₅	5	8194.9431(35)		5 ₄₁	4	4 ₃₂	3

^a *F** = *F* + 1/2. All frequencies are in MHz with listed 1σ uncertainties in the last significant digits.

changes in the Fe–Br bond length, with the bond remaining in the *ac* plane; (ii) changes in the distance of the allyl group from the rest of the molecule; (iii) expansion or contraction of the

allyl group while maintaining *C*_s symmetry; (iv) changes in the Fe–C(equatorial carbonyls) while maintaining *C*_s molecular symmetry; (v) motion of the axial carbonyl group within the

Table 3. Measured Transition Frequencies for the ^{54}Fe , ^{79}Br Isotopomer of *anti*- $\text{C}_3\text{H}_5\text{Fe}(\text{CO})_3\text{Br}^a$

$^{79}\text{Br } ^{54}\text{Fe}$	J'_{K_p, K_o}	$F^{*'} $	J_{K_p, K_o}	F^*
5196.8949(15)	3 ₃₀	5	2 ₂₀	4
5196.8949(15)	3 ₃₁	5	2 ₂₁	4
5811.2622(34)	5 ₃₃	7	4 ₃₂	6
5811.2622(34)	5 ₃₂	7	4 ₃₁	6
5834.3041(90)	5 ₂₄	6	4 ₂₃	5
5834.4110(22)	5 ₂₃	6	4 ₂₂	5
5836.5097(56)	5 ₃₂	5	4 ₃₁	4
6918.0799(08)	4 ₄₀	5	3 ₃₀	5
7022.0917(47)	4 ₄₀	5	3 ₃₀	4
7022.0917(47)	4 ₄₁	5	3 ₃₁	4
7034.7755(15)	4 ₄₀	6	3 ₃₀	5
7034.7755(15)	4 ₄₁	6	3 ₃₁	5
7062.3558(48)	4 ₄₀	4	3 ₃₀	4
7062.3558(48)	4 ₄₁	4	3 ₃₁	4
8152.5724(58)	7 ₂₅	5	6 ₂₄	5
8156.2691(69)	7 ₀₇	7	6 ₀₆	6
8156.3168(64)	7 ₀₇	6	6 ₀₆	5
8157.6017(13)	7 ₂₆	8	6 ₂₅	7

^a $F^* = F + 1/2$. All frequencies are in MHz with listed 1 σ uncertainties in the last significant digits.

Table 4. Measured Transition Frequencies for the ^{54}Fe , ^{81}Br Isotopomer of *anti*- $\text{C}_3\text{H}_5\text{Fe}(\text{CO})_3\text{Br}^a$

$^{81}\text{Br } ^{54}\text{Fe}$	J'_{K_p, K_o}	$F^{*'} $	J_{K_p, K_o}	F^*
5180.0962(29)	3 ₃₀	2	2 ₂₀	1
5180.0962(29)	3 ₃₁	2	2 ₂₁	1
5251.6270(17)	3 ₃₁	2	2 ₂₁	2
5251.6270(17)	3 ₃₁	2	2 ₂₁	2
5764.4174(59)	5 ₃₃	7	4 ₃₂	6
5764.4174(59)	5 ₃₂	7	4 ₃₁	6
5769.4858(22)	5 ₁₅	7	4 ₁₄	6
5777.1810(20)	5 ₁₄	7	4 ₁₃	6
5779.0700(52)	5 ₀₅	4	4 ₀₄	3
5780.5638(23)	5 ₁₄	6	4 ₁₃	5
5782.0805(64)	5 ₂₃	5	4 ₂₂	4
5783.7252(28)	5 ₂₄	6	4 ₂₃	5
5783.8292(16)	5 ₂₃	6	4 ₂₂	5
5785.4853(13)	5 ₃₃	5	4 ₃₂	4
5785.4853(13)	5 ₃₂	5	4 ₃₁	4
6923.8530(37)	6 ₃₄	8	5 ₃₃	7
6930.273(12)	4 ₄₀	5	3 ₃₀	5
6935.2581(47)	6 ₂₅	6	5 ₂₄	5
6935.2811(67)	6 ₂₄	7	5 ₂₃	6
6935.4246(51)	6 ₂₄	6	5 ₂₃	5
6935.8345(53)	6 ₁₅	7	5 ₁₄	6
6937.9713(27)	6 ₃₄	6	5 ₃₃	5
6937.9713(27)	6 ₃₃	6	5 ₃₂	5
6938.2123(48)	6 ₁₅	6	5 ₁₄	5
6941.6185(34)	6 ₃₄	7	5 ₃₃	6
6941.6185(34)	6 ₃₃	7	5 ₃₂	6
8176.8456(23)	5 ₄₂	5	4 ₃₂	5

^a $F^* = F + 1/2$. All frequencies are in MHz with listed 1 σ uncertainties in the last significant digits.

symmetry plane. The crystal structure was used as the initial structure, but it was modified to include the H1 atom and to require linear Fe–C–O angles. The C–O distance was fixed at 1.145 Å. The *a* and *c* coordinates of the allyl group are constrained such that the tilt angle of the allyl carbon atoms also remains close to the X-ray value of 86°. This parameter set allows subtle changes of the (solid-state) molecular structure that give a gas-phase structure in better agreement with the microwave data. Parameters one through four and six can be fit with just the ^{79}Br and ^{81}Br data set (six constants) to give a reasonable structure. Inclusion of the ^{54}Fe data allowed the remaining parameters to be varied, although they did not change much from the X-ray values. The coordinates obtained from the fit described here are shown in Table 9, and heavy-atom

Table 5. Spectral Parameters for the Anti Isomer of $\text{C}_3\text{H}_5\text{Fe}(\text{CO})_3\text{Br}$ Derived from the Measured Spectra^a

param	unit	anti ^{79}Br	anti ^{81}Br	anti $^{79}\text{Br}^{54}\text{Fe}$	anti $^{81}\text{Br}^{54}\text{Fe}$
<i>A</i>	MHz	920.6148(2)	920.5990(2)	920.6120(2)	920.5099(2)
<i>B</i>	MHz	582.8866(12)	577.9610(16)	583.2816(3)	578.3750(3)
<i>C</i>	MHz	581.3027(12)	576.3847(16)	581.7073(3)	576.8011(3)
χ_{aa}	MHz	334.964(2)	279.889(3)	335.296(3)	280.006(9)
$\chi_{bb} - \chi_{cc}$	MHz	-2.007(11)	-1.719(10)	-2.007(f)	-1.719(f)
$ \chi_{ac} $	MHz	46.4(3)	36.7(3)	46.4(f)	36.7(f)
<i>D_J</i>	Hz	27(1)	25(1)	27(f)	25(f)
<i>D_{JK}</i>	Hz	68(4)	61(5)	68(f)	61(f)
<i>D_K</i>	Hz	-39(11)	-23(11)	-39(f)	-23(f)
δ_J	Hz	6(2)	10(2)	6(f)	10(f)
δ_K	kHz	5.1(6)	7.8(8)	5.1(f)	7.8(f)
σ	kHz	5.1	4.3	7.0	11.0
no. of lines		168(144)	129(114)	16(11)	28(21)

^a (f) indicates that the parameter was fixed. the number of assigned components is the first entry in the no. of lines row, and the number in parentheses is the number of fully resolved lines.

Table 6. Spectral Parameters for the Syn Isomer of $\text{C}_3\text{H}_5\text{Fe}(\text{CO})_3\text{Br}$ Derived from the Measured Spectra

parameter	unit	syn ^{79}Br	syn ^{81}Br
<i>A</i>	MHz	919.506(1)	919.484(1)
<i>B</i>	MHz	584.187(3)	579.222(3)
<i>C</i>	MHz	579.639(3)	574.742(3)
χ_{aa}	MHz	349.910(5)	292.323(6)
$\chi_{bb} - \chi_{cc}$	MHz	-12.388(20)	-10.29(12)
$ \chi_{ab} $	MHz	36.4(10)	28.9(11)
<i>D_J</i>	Hz	20(1)	19(1)
<i>D_{JK}</i>	Hz	119(2)	104(2)
σ	kHz	4.4	6.6
no. of lines		104(80)	74(60)

Table 7. Cartesian Coordinates of *anti*- $\text{FeC}_3\text{H}_5(\text{CO})_3\text{Br}$ Calculated Using Gaussian BPW91/6-311G

atom	<i>a</i> (Å)	<i>b</i> (Å)	<i>c</i> (Å)
Br	-1.9722	0.0000	0.1356
Fe	0.6016	0.0000	0.0693
C1	0.7524	-1.2404	1.8362
C2	1.4146	0.0000	2.0260
C3	0.7524	1.2404	1.8362
H1	2.5046	0.0000	2.0939
H2	-0.2909	-1.3687	2.1143
H3	1.3543	-2.1471	1.8264
H4	-0.2909	1.3687	2.1143
H5	1.3543	2.1471	1.8264
C4	0.1693	-1.4065	-0.9457
C5	2.2662	0.0000	-0.4612
C6	0.1693	1.4065	-0.9457
O1	-0.0954	2.3494	-1.5971
O2	3.3814	0.0000	-0.8560
O3	-0.0954	-2.3494	-1.5971

internal coordinates are given in Table 10. It is interesting to note that the structural parameters for the allyl ligand in this complex are very close to the values for the free allyl radical.⁵ For the anti isomer, the C–C–C interbond angle is 125(1)°, whereas it is 124° in the free allyl radical. The C–C bond is 1.396(11) Å in the complex and 1.387 Å in allyl radical. A comparison of the least-squares-fit (LSQ), theoretical (DFT), and solid-state (X-ray) structural parameters is shown in Table 10.

Using *anti*- $\text{C}_3\text{H}_5^{56}\text{Fe}(\text{CO})_3\text{Br}$ as the “parent” and *anti*- $\text{C}_3\text{H}_5^{56}\text{Fe}(\text{CO})_3^{81}\text{Br}$ and *anti*- $\text{C}_3\text{H}_5^{54}\text{Fe}(\text{CO})_3^{79}\text{Br}$ as substituted species the r_s value for the Fe–Br bond length in the anti conformation can be determined. The *a* axis is nearly coincident with the Fe–Br bond, and thus b_s and c_s coordinates for these atoms are small and not well determined. The two a_s coordinates are $a_s(\text{Fe}) = 0.545$ Å and $a_s(\text{Br}) = 1.932$ Å. Placement of the center of mass between these two atoms results in an $r_s(\text{Fe} -$

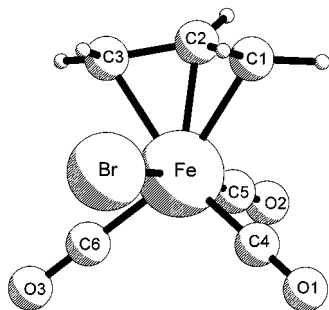


Figure 2. Structure of *anti*-allyltricarbyliron bromide, indicating the numbering of the carbon atoms used in the data analysis.

Table 8. Cartesian Coordinates of *syn*-FeC₃H₅(CO)₃Br Calculated Using Gaussian BPW91/6-311G

atom	<i>a</i> (Å)	<i>b</i> (Å)	<i>c</i> (Å)
Br	-1.9766	0.1297	0.0000
Fe	0.5854	0.0606	0.0000
C1	1.1187	1.7748	-1.2427
C2	0.5718	2.1811	0.0000
C3	1.1187	1.7748	1.2427
H1	-0.4356	2.5894	0.0000
H2	2.1956	1.7115	-1.3957
H3	0.5370	1.9572	-2.1443
H4	2.1956	1.7115	1.3957
H5	0.5370	1.9572	2.1443
C4	0.1823	-0.9707	-1.3988
C5	2.2710	-0.4008	0.0000
C6	0.1823	-0.9707	1.3988
O1	-0.0500	-1.6391	-2.3387
O2	3.4034	-0.7417	0.0000
O3	-0.0500	-1.6391	-2.3387

Table 9. Best-Fit Coordinates for the Partial Structure Determination of *anti*-C₃H₅Fe(CO)₃Br^a

atom	<i>a</i> ₀ (Å)	<i>b</i> ₀ (Å)	<i>c</i> ₀ (Å)
Br	-1.9324(19)	0.0000	0.0833(47)
Fe	0.5394(52)	0.0000	0.0551(55)
C1	0.4756(56)	-1.2383(60)	1.8190(38)
C2	1.0700(56)	0.0000	2.0661(38)
C3	0.4756(56)	1.2383(60)	1.8190(38)
H1	2.0588(56)	0.0000	2.4773(38)
H2	-0.3979(56)	-1.1931(60)	1.9426(38)
H3	0.8958(56)	-2.2303(60)	1.7735(38)
H4	-0.3979(56)	1.1958(60)	1.9426(38)
H5	0.8958(56)	2.2277(60)	1.7735(38)
C4	0.3003(54)	-1.4407(16)	-1.0264(35)
C5	2.3186(50)	0.0000	-0.2140(60)
C6	0.3003(54)	1.4407(16)	-1.0264(35)
O1	0.1514(54)	-2.3466(16)	-1.7106(35)
O2	3.4463(50)	0.0000	-0.3855(60)
O3	0.1514(54)	2.3466(16)	-1.7106(35)

^a The standard deviation of the fit is 0.026 amu Å². Errors listed are 1σ and do not reflect possible additional errors due to the assumptions of structural integrity of the ligands or possible correlations between parameters.

Br) bond length of 2.477 Å. This value is significantly shorter than the value obtained with DFT ($r_e = 2.575$ Å) but much closer to the X-ray value of 2.494 Å. It is likely that small displacements of Fe and Br (more likely Br) from the *a* axis that are neglected here would increase $r_s(\text{Fe}-\text{Br})$ slightly, and then it would be in even better agreement with the X-ray value.

Structural Considerations for the Syn Conformation

For the *syn* isomer, only six rotational constants are presently available, and therefore, the structural analysis is much more limited than for the *anti* isomer. There was no previously

Table 10. Internal Coordinates of *anti*-Allyltricarbyliron Bromide^a

coord	LSQ	DFT	X-ray
$r(\text{Fe}-\text{Br})$	2.472(9)	2.575	2.494
$r(\text{Fe}-\text{C1},3)$	2.156(11)	2.164	2.129
$r(\text{Fe}-\text{C2})$	2.080(12)	2.119	2.058
$r(\text{Fe}-\text{C4},6)$	1.817(7)	1.788	1.786
$r(\text{Fe}-\text{C5})$	1.800(12)	1.747	1.790
$r(\text{C1}-\text{C2},3)$	1.396(11)	1.419	1.392
$\angle(\text{Br}-\text{Fe}-\text{C5})$	172.1(7)	170.0	171.9
$\angle(\text{C1}-\text{C2}-\text{C3})$	125.1(9)	121.9	124.9
$\angle(\text{C4}-\text{Fe}-\text{C5})$	104.9(5)	103.8	105.9
$\angle(\text{Br}-\text{Fe}-\text{C4},6)$	82.8(4)	80.6	83.5
$\angle(\text{C3}-\text{C2}-\text{Fe}-\text{Br})$	67.5(10)	66.5	67.7

^a Bond lengths are in Å, and interbond angles in deg. The X-ray values are from ref3.

Table 11. Quadrupole Coupling Tensor Elements in the Principal Inertial Axis System (*abc* System) and in the Principal Axis System of the Quadrupole Coupling Tensor (*xyz* System)^a

param	<i>anti</i> ⁷⁹ Br	<i>anti</i> ⁸¹ Br	<i>syn</i> ⁷⁹ Br	<i>syn</i> ⁸¹ Br
χ_{aa}	334.964	279.889	349.910	292.323
χ_{bb}	-168.486	-140.804	-181.149	-151.307
χ_{cc}	-166.479	-139.085	-168.761	-141.017
χ_{xx}	-170.736	-142.275	-183.632	-153.181
χ_{yy}	-168.486	-140.804	-168.761	-141.017
χ_{zz}	339.221	283.079	352.393	294.198
$ \theta $	5.3(3)	5.0(3)	3.9(3)	3.7(3)
η	-0.0066	-0.0052	-0.0422	-0.0413
$(^{79}\text{Br})\chi_{yy}/(^{81}\text{Br})\chi_{yy}$	1.1966(1)		1.1967(3)	

^a The coordinate *x* corresponds to *c* for *anti* and *x* corresponds to *b* for *syn*. These coordinates and the *a* and *z* coordinates lie in the symmetry plane of the molecule. The *y* coordinates are perpendicular to this symmetry plane. The Coordinate *y* = *b* for *anti* and *y* = *c* for *syn*. The quadrupole asymmetry parameter, η , is given by $(\chi_{xx} - \chi_{yy})/\chi_{zz}$. The off-diagonal components (χ_{ac} for *anti*, and χ_{ab} for *syn*) are given in Tables 5 and 6.

reported structure for this isomer, so the present DFT structure is used as a reference. The DFT calculations indicate that rotating and tilting the allyl group to form the *syn* isomer causes a switch of the *b* and *c* inertial axes. This small displacement of the center of mass of the allyl group upon isomerization can cause the unexpected axis change only because the two conformations are *both* near symmetric tops. The *anti* isomer, had $B-C \sim 1$ MHz. The switch to the *syn* conformation decreased *B* more than *C* and, therefore, caused exchange of the principal axes (by definition) and a consequential change from *c* type dipole to *b* type dipole selection rules.

Quadrupole Coupling

The quadrupole coupling parameters in the principal quadrupole axis systems of the two isomers are given in Table 11. We note that the *bb* (*yy*) components of the *anti* isomer tensors are nearly equal to the corresponding *cc* (*yy*) components of the *syn* isomer tensors for each isotopomer. This is strong support for the switch in inertial axis assignments between the two isomers. For each isomer, either *b* (or *c*) dipole transitions are assignable to the (non-*a* type) lines. Either assignment gives the same quadrupole coupling tensor, to within quoted error limits. Due to the symmetry plane present in both isomers, and the identical connectivity (i.e. an Fe-Br bond), the isomers would be expected to have very similar values for the *yy* component of the quadrupole tensor that is normal to the symmetry plane. This axis will not rotate due to 180° rotation of the allyl group (isomerization) or isotopic substitution in the symmetry plane.

The experimental quadrupole coupling tensor in the *abc* inertial axis system was diagonalized to obtain the following: (1) the principal axis values in the principal axis system for the quadrupole coupling tensor (*xyz* axis system); (2) the angles between axes in the two coordinate systems. The quadrupole components in both the *abc* system and *xyz* system and the asymmetry parameters, $\eta = (\chi_{xx} - \chi_{yy})/\chi_{zz}$, are listed in Table 11. The *y* axis is chosen to be perpendicular to the mirror plane of the molecule. For the anti isomer, the transformation from the *abc* to *xyz* system is a rotation about the *b* axis by $|\theta| \cong 5^\circ$. For the syn isomer, this transformation is a rotation about the *c* axis by $|\theta| \cong 4^\circ$. The *a* axis is very nearly aligned with the Fe–Br bond, so these values for θ indicate a smaller rotation of the quadrupole tensor principal axis away from the Fe–Br bond direction for the syn isomer. We can compare differences in the *xyz* system quadrupole components which are perpendicular to the axis most nearly aligned with the Fe–Br bond. These differences would be zero for a symmetric top, and in this near symmetric top molecule, the numbers are small but nonzero. Clearly the accuracies of the principal quadrupole components are limited by the accuracy of the off-diagonal parameter, the most poorly determined parameter from fits to the spectrum. It was interesting to note that the asymmetry parameter, η , is different for the two structural isomers. Since both isomers have the same connectivity (i.e. an Fe–Br bond), it was somewhat unexpected to see such a significant change in the Fe–Br bonding upon rearrangement of the allyl group. Qualitative molecular orbital plots based on DFT calculations at the STO-3G level give a possible explanation of this behavior. The highest and second-highest occupied molecular orbitals of the two conformations are primarily $p_x(\text{Br})$ and $p_y(\text{Br})$ character. The calculations suggest that, upon isomerization, the energy ordering of these orbitals switches with the orientation of the allyl group.

Discussion

The measured transition intensities for the two isotopomers of bromine for each isomer were approximately equal in magnitude. Fewer transitions were measured for the ^{81}Br transitions only because the entire spectrum was not scanned. Typically, the *a* dipole ^{79}Br transitions overlapped the *a* dipole ^{81}Br transitions at lower frequencies and *b* or *c* dipole type transitions for both isomers and isotopes at higher frequencies. Because of the larger variety of lines at higher frequencies in the scanned regions, these regions were studied more closely than the lower frequency regions that contained the extra *a* type transitions for the ^{81}Br isotopomers. Since the *b* (or *c*) type transitions available in this frequency region have lower values for *J*, *K*, and *F*, they are somewhat better probes of the quadrupole coupling tensors of these molecules. Considerably more effort was put into measurement of these transitions, as opposed to the abundance of easily measurable high-*J*, *a* type transitions. Without *b* or *c* type transitions in the spectral fits, the value of *B* – *C* would have been completely undetermined, and similarly, fitting only *b* or *c* type transitions does not allow an accurate value of *B* (or *C*, respectively) to be determined. Only a combination of both types of transitions allowed independent determination of all the rotational constants in the species.

Since the Br atom is generally considered a single electron donor with filled *p* orbitals, any differences in p_x and p_y orbital populations would indicate either a π interaction with the metal center or a nonbonding interaction that perturbs the *p* orbitals in different ways. Photoelectron spectra studies¹³ indicate that small π interactions of the bromine atom with the iron atom

Table 12. Comparison of Measured (MW) and Calculated (DFT) Parameters for the Main Isotopomer $\text{C}_3\text{H}_5^{56}\text{Fe}(\text{CO})_3^{79}\text{Br}^a$

param	anti MW	anti DFT	syn MW	syn DFT
A (MHz)	920.6148(2)	921.816	919.5055(1)	919.051
B (MHz)	582.8866(12)	565.945	584.1865(1)	567.358
C (MHz)	581.3027(12)	565.840	579.6392(1)	563.856
κ	–0.9908	–0.9994	–0.9732	–0.9803
INT/energy	1	0.0 cm^{-1}	0.1	609 cm^{-1}

^a κ is Ray's asymmetry parameter with –1.0 indicating a prolate symmetric top. Intensity (INT) is rough average of the normalized syn spectrum. Energy is in wavenumbers relative to the calculated minimum energy of the syn conformation.

may be expected. In a photoelectron study of pentacarbonyl-rhenium halides,¹³ a filled-filled π donation is shown to be more important for the lighter halogen chlorine and less important for iodine. For discussion of the orbital interactions, the *z* axis is aligned with the Fe–Br bond and the *x* axis points toward the allyl ligand. This corresponds to the definitions for the principal quadrupole axes in the last section. All orbitals in this discussion refer to the valence shells of Fe and Br. The $p_x(\text{Br})$ orbital can interact with the $d_{xz}(\text{Fe})$ as can the $p_y(\text{Br})$ and the $d_{yz}(\text{Fe})$ orbitals. Plots of the HOMO and SHOMO (second-highest occupied molecular orbital) both contain mostly bromine *p* character and some iron *d* character (along with allyl character). This suggests that the change of the asymmetry of the electric field gradient upon isomerization may be attributed to a change in metal orbital character which, in turn, can be influenced by other ligands such as the allyl group. In both isomers, anti or syn, a splitting of the metal d_{xz} and d_{yz} orbitals occurs due to the presence of the allyl ligand (these would be degenerate in a symmetric system such as $\text{BrRe}(\text{CO})_5$ or the radical $\text{BrFe}(\text{CO})_4$). This symmetry reduction at the metal center is caused by both the electronic and geometric perturbations in the molecule. The bonding between iron and bromine is primarily a σ interaction between the $p_z(\text{Br})$ (or sp_z hybrid) and $d_{z^2}(\text{Fe})$. This interaction alone would result in a cylindrically symmetric electric field gradient at the Br nucleus and thus an asymmetry (η) of zero. However, as indicated by these measurements of the electric field gradient at the Br nucleus, η is not zero. On the basis of the known propensity of Br to interact with metal *d* orbitals through π bonding, this asymmetry can be at least partially attributed to the nonequivalence of the d_{xz} and d_{yz} orbitals caused by the presence of the allyl ligand. Although small, this subtle interaction is observable, and the change in electric field gradient asymmetry appears to be correlated to the reorientation of the allyl ligand.

A nonbonding, or electrostatic, interaction may also contribute to the observed electric field gradient asymmetry. In some systems, polarization of the valence shell of a quadrupolar nucleus from electrostatic forces causes changes in the electric field gradient at the quadrupolar nucleus of up to 2%.¹⁴ We note that the allylic protons H1 and H2, H4 in complimentary isomers can each approach the Br atom to within ~ 2.7 Å. Note the geometric arrangement of these hydrogen atoms with respect to the bromine atom. In the syn isomer the H1 proton lies in the symmetry plane and can potentially interact with the p_x orbital. In the anti isomer the H2 and H4 protons lie 1.37 Å on either side of the mirror plane. These protons would be expected to have less interaction with the p_x orbital of Br. Such a nonbonding interaction of the bromine with the allyl ligand may

(13) Hall, M. B. *J. Am. Chem. Soc.* **1975**, 97 (8), 2057.

(14) Townes, C. H.; Schawlow, A. L. *Microwave Spectroscopy*; Dover Press: New York, 1975.

also contribute to the observed change in the quadrupole coupling asymmetry.

Conclusions

Two gas-phase conformations of allylirontricarboylbromide have been identified and characterized using microwave spectroscopy and DFT calculations. A thorough analysis of the moments of inertia and elements of the bromine quadrupole coupling tensors is given. The anti conformation is identified as the major component of the gas-phase samples. The important structural parameters of the anti conformation are well-determined using measured moments of inertia and a partial least-squares structure fit. This gas-phase structure for the anti conformation is in good agreement with present DFT calculations and previous X-ray work. A reasonable assignment of a second isomer to the syn conformation is obtained, on the basis of comparisons of microwave and DFT data, as shown in Table 12. The DFT calculations suggest a switch of the *b* and *c* inertial axes upon isomerization, and this is supported by the measured

quadrupole coupling data. Furthermore, changes in the measured rotational constants agree well with the calculated values, especially with the slightly larger deviation from a symmetric top for the syn conformation. Finally, the spectrum assigned to the syn conformation is much weaker (by a factor of 10) than that assigned to the anti conformation. This is in good agreement with the DFT results, which predict a lower energy (by 609 cm^{-1}) for the anti conformation. This is also in agreement with the NMR data which indicate stronger signals for the anti conformation. Since both isomers are observed in the cold (10–15 K) molecular beam, it appears that the isomer states have not had sufficient time to come into equilibrium with the rotational (and translational) temperature of the beam, in the brief expansion time, before the molecules are too far apart for further interaction.

Acknowledgment. We thank the National Science Foundation (Grant CHE-9634130) for support of this research.

IC990884R